ICONHIC 2016
1st International Conference on Natural Hazards & Infrastructure
28-30 June, 2016, Chania, Greece

Effect of Imperfect Contact on the Response of Suction Caissons for Offshore Wind Turbines

I. Georgiou[1], P. Lekkakis, R. Kourkoulis, F. Gelagoti, G. Gazetas
National Technical University of Athens

ABSTRACT

In pursuit of Performance Based Design of the challenging offshore infrastructure, this paper investigates the stiffness coefficients of suction caisson foundations both in the elastic domain and when considering material and geometrical nonlinearities, using three-dimensional finite-element analyses. As an extension of previous work, expressions from the literature are modified to identify the elastic stiffness matrix of solid circular foundations embedded in homogeneous soil. Taking into account the skirt flexibility, a reduction factor was engendered which yields the stiffness of a flexible skirted foundation as a proportion of the corresponding stiffness of the solid counterpart, for different embedment ratios. In the second part of the study, charts for the non-linear stiffness coefficients were produced, allowing the calculation of the stiffness degradation with increasing rotations and displacements, while highlighting the effect of the soil-sidewalls interfaces. It is shown that imperfect interfaces may substantially reduce the stiffness of the soil-foundation system, even for relatively small rotations and displacements. Reduced interface shear resistance proved more crucial than the tensionless interface scenario in terms of stiffnesses, while the reversed trend is observed for the maximum capacities.

Keywords: suction caisson, stiffnesses, numerical modeling, imperfect interfaces

INTRODUCTION

Installation of offshore wind farms is increasingly planned worldwide to exploit the enormous energy potential associated with the vast offshore areas and the consistently stronger winds compared to their onshore counterparts. Among a variety of conventional foundation schemes (shallow footings, monopiles, tripods etc.) that have been utilized so far, skirted circular foundations (commonly referred to as “suction caissons” or “bucket foundations” by the offshore industry) are gaining popularity as an easy-to implement solution. Their principal advantage is the ease of the installation process, which consists of floating the caisson to its location, where it is driven into the seabed under the action of its self-weight and pumping of water trapped within the skirts. The differential pressure due to pumping creates suction which attracts the caisson lid downwards until attaining full contact with the soil. Compared to simple raft or massive embedded foundations, suction caissons are supposed to possess the additional benefit of resisting uplift (through the development of suction) and are thus regarded as more effective alternative to the monopile solution for offshore wind turbines, where large overturning moments govern the foundation response (e.g. Clukey & Morrison, 1993; Tani & Craig, 1995; Bransby & Randolph, 1998; Byrne, 2000; Houlsby et al., 2005; Gourvenec, 2007; Bransby & Yun, 2009).

Extensive research on the response of skirted foundations has been conducted so far by means of numerical studies (Bransby & Yun, 2009; Gourvenec, 2008; Ukritchon et al., 1998; Taiebat & Carter, 2000; Gourvenec & Barnett, 2011; Vulpe, 2015). The majority of these studies have focused mainly on the undrained bearing

[1] Corresponding Author: I.A. Georgiou, *National Technical University of Athens, irelimni@outlook.com*

capacity under combined loading taking into account the effect of foundation geometry, foundation embedment ratio and soil heterogeneity. As such, they have developed failure envelopes either assuming that the soil compartment acts as a rigid body; thus modelling an embedded foundation or a surface foundation able to resist unlimited tension; or physically modelling the caisson skirts in plain strain conditions (Bransby & Yun, 2009; Gourvenec & Barnett, 2011; Barari & Ibsen, 2012) as well as in the three-dimensional space (Kourkoulis et al, 2014; Vulpe, 2015). Furthermore, most studies on suction caisson foundations on clay tend to consider full contact conditions between the foundation and the soil, in other words the detachment of the soil of the caisson is prevented and the soil-caisson interface is assumed to be rough is shear. To the author's knowledge, only limited case studies where imperfect interfaces of skirted foundations are implemented were analyzed; Kourkoulis et al. (2014) evaluated the effect of soil-sidewall interfaces under monotonic lateral, cyclic and earthquake loading, while Vulpe (2015) investigated the effect of soil-skirt interface on the combined capacity of skirted circular foundations.

However, the prediction of the performance of offshore structures under environmental loading requires knowledge of the elastic or quasi-elastic stiffnesses of the foundation, since these control the natural frequencies of the system, and hence the loads that are transmitted from the structure to the foundation. Various publications in the past decades have tackled the subject of elastic static or dynamic stiffnesses for various foundation shapes and types. (Poulos & Davis, 1974; Gazetas, 1983, 1987, 1991; Roesset, 1980; Doherty & Deeks, 2003, 2005; Doherty et al., 2005). As far as the suction caisson is concerned, little work has been conducted to define the elastic or nonlinear stiffness coefficients of the soil-foundation system. Doherty & Deeks (2003) firstly managed to calculate the elastic stiffnesses for a rigid caisson. Expanding that work, Doherty et al. (2005), using a scaled boundary finite element method, proposed a simple methodology through which the elastic stiffnesses of flexible skirted foundations could be expressed, for homogeneous and different profiles of inhomogeneous elastic soil half-space. Liingaard et al. (2007), using a coupled boundary element/finite element method, managed to provide tables with non-dimensional values of the static stiffnesses of a suction caisson, much like Doherty et al. (2005), but also took the problem a step further by investigating the impedance of suction caissons, in vertical and sliding-rocking vibrations.

Based on the above background, the aim of the current study is to extend previous work in an effort to investigate the overall monotonic load-displacement response of suction caissons. Elastic and non-linear three dimensional finite elements will be used in order to parametrically evaluate the effects of soil-sidewalls interfaces and of skirt flexibility both in small and large strain domain.

PROBLEM DESCRIPTION AND NUMERICAL MODELING

The foundation under study refers to a circular suction caisson of diameter D embedded into soil at depth L. The L/D ratio has been varied parametrically so as to represent three characteristic alternatives: a shallow caisson with L/D=0.2, an intermediate case (L/D=0.5), and a deeply embedded alternative of L/D=1. The foundations are lying on a homogeneous clay deposit of uniform undrained shear strength (s_u).

The analyses for the investigation of the problem were conducted in three-dimensional space using the finite element code ABAQUS. The developed FE model for a foundation with embedment ratio L/D=0.2 is displayed in Fig. 1. A similar mesh discretization was adopted for the meshes for each of the different embedment ratios, maintaining a constant width and adjusting the mesh in the vertical direction. The soil body was modelled using eight-node hexahedral continuum elements (C3D8), obeying to a kinematic hardening constitutive model with Von Mises failure criterion (Anastasopoulos et al., 2012), while the foundation was modelled using linear elastic shell elements. A very fine discretization has been adopted for the first 8 layers of circumferential elements in the region of the soil-foundation interface (which were found to control the FE predictions of the foundation lateral response), while to increase computational efficiency, mesh coarseness increases away from the foundation. External boundaries were set sufficiently remotely from the foundation to ensure no boundary effects on the foundation response (radius and height of the model equal to 3D and 2.5D respectively).

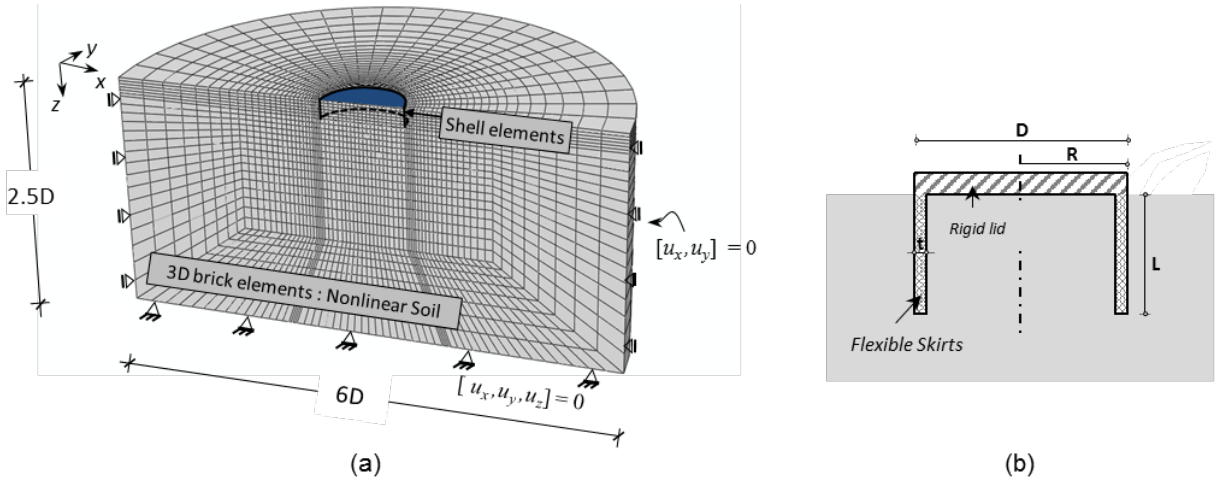

Figure 1. (a) Finite element mesh (a half-model section is presented); (b) Caisson foundation geometry and adopted notation

It is widely accepted that due to several factors, usually relative to suction caisson installation process or to the multitude of loading cycles during the lifetime of a wind turbine, the soil-caisson foundation interface conditions may not always be approximated as fully bonded (Randolph & House, 2012; Gourvenec et al., 2009). In order to simulate as realistically as possible the contact conditions between the foundation and the surrounding soil, special contact elements are introduced. As it is impossible to estimate the proportion of the residual interface strength a priori, its effect is herein investigated parametrically by means of the following three assumptions:

- *Full Contact* scenario, where the interface is rough in shear and has infinite tensile capacity
- *Frictionless* scenario, in which case the interface is considered fully smooth (zero shear resistance), while the soil has infinite tensile capacity (no separation allowed). This scenario was considered to provide a lower limit to the overall response, since in reality a level of frictional contact is expected between the soil and the outer wall of the skirts.
- *Tensionless* scenario, where separation (gapping) of the foundation from the surrounding soil is permitted, and the maximum shear resistance is the undrained soil shear strength (s_u)

ELASTIC STIFFNESSES OF SUCTION CAISSONS

The expressions that have been formed in previous works for embedded foundations are all for a reference point at the bottom of the foundation (i.e. the skirt tip level). In producing relationships between embedded and skirted foundations, this would be inconvenient since the skirts are also flexible and the relative position of the reference point (with the exception of fully rigid skirts) would change depending on the degree of flexibility. Moreover, loading from wind turbines is transmitted from the turbine tower to the caisson top, and separation of the latter from the soil may modify the amount of loading imparted to its base. Thus, the first step in deducing these expressions must be the translation of the load reference point to the top of the foundation (i.e. the center of the foundation lid), which is considered rigid in all cases.

Table 1. Elastic Stiffnesses for circular surface foundations

	Gazetas (1991)	**Deviation**
K_V	$\frac{8GR}{2-v}\left(1+\frac{1}{2}\frac{R}{H}\right)$	7%
K_H	$\frac{8GR}{2-v}\left(1+\frac{1}{2}\frac{R}{H}\right)$	2%
K_R	$\frac{8GR^3}{3(1-v)}\left(1+\frac{1}{6}\frac{R}{H}\right)$	0.8%
K_T	$\frac{16}{3}GR^3\left(1+\frac{1}{12}\frac{R}{H}\right)$	0.9%

Before proceeding to the proposed stiffness coefficients, the adopted numerical model is validated against published expressions for the elastic stiffnesses of a circular surface foundation lying on a homogeneous soil deposit (Gazetas, 1991). It can be seen from Fig. 2 that there is excellent agreement between the stiffness coefficients computed directly and the solutions obtained from the expressions in Table 1. Having validated the numerical model, a new set of finite element analyses was conducted with different foundation radii and depths for the "rocky substratum", where the response of the fully rigid caisson was investigated in the elastic domain. Based on the above analyses, the following propositions are made to modify the classical expressions into simpler and more accurate ones in order to estimate the response of the solid embedded cylindrical caisson with the load reference point at the top of the foundation:

$$K_V = \frac{4GR}{1-\nu}\left(1 + 1.6\frac{R}{H}\right)\left(1 + 0.4\frac{L}{R}\right)\left[1 + \left(0.9 - 0.25\frac{L}{R}\right)\frac{L}{H-L}\right] \quad (1)$$

$$K_H = \frac{8GR}{2-\nu}\left(1 + 0.7\frac{R}{H}\right)\left(1 + 1.1\left(\frac{L}{R}\right)^{0.65}\right)\left(1 + 1.15\ \frac{L}{H}\right) \quad (2)$$

$$K_R = \frac{8GR^3}{3(1-\nu)}\left(1 + 0.15\frac{R}{H}\right)\left[1 + 0.95\frac{L}{R}\left(1 + \frac{L}{R}\right)^{1.4}\right]\left(1 + 0.7\frac{L}{H}\right) \quad (3)$$

$$K_C = 0.6\ K_H L \quad (4)$$

$$K_T = \frac{16}{3}GR^3\left(1 + \frac{1}{12}\frac{R}{H}\right)\left[1 + 2.7\left(\frac{L}{R}\right)^{0.9}\right] \quad (5)$$

In Table 2 the maximum deviations of the new functions from the finite element analysis results are presented. The accuracy of the results is certainly contingent on various parameters, such as the mesh refinement and the distance of the external boundaries. The models used for the estimation of the system were designed in such a way so as to minimize as much as possible the effect of these parameters.

Table 2. Expressions for solid cylindrical foundations: maximum percentile differences from FE results

	$\mathbf{K_V}$	$\mathbf{K_H}$	$\mathbf{K_R}$	$\mathbf{K_C}$	$\mathbf{K_T}$
This study	3.7%	2.6%	3.7%	6.6%	1.1%

Having defined suitable expressions for the elastic stiffness coefficients of cylindrical solid caissons, the second part of the process of deriving expressions for skirted foundations is to find a dimensionless parameter that will be able to produce unique stiffness values for differing soil conditions and skirt flexibility. The lid of the suction caisson is considered rigid (usually a stiffened steel structure); hence, if the skirts have a very small thickness or elastic modulus, the foundation will behave like a surface footing. Similar to the dimensionless parameter J defined by Doherty et al. (2005), a new parameter is introduced as follows:

$$\mathfrak{J} = \frac{E_{steel}\ t}{E_{soil}\ D} \quad (6)$$

where E_{steel} the elastic modulus for steel (usually 210GPa), t the skirt thickness, E_{soil} the Young's modulus for the soil and D the foundation diameter. By conducting several analyses where one of the above parameters was varied while the rest remained constant, it was found that indeed unique stiffnesses were defined by the value of $\mathfrak{J}$ (deviation of 2% at most). Additionally, for very small values of $\mathfrak{J}$ the stiffness coefficients reduced to those for a surface foundation. Conversely, for very large values of $\mathfrak{J}$ the stiffness coefficients are practically equal (difference of 3-4% for large embedment ratios) with those of an equivalent solid embedded foundation. The purpose is to elicit a "reduction" factor which when multiplied with the stiffness of the solid foundation would yield the stiffness of the equivalent skirted foundation. Therefore, the results presented are in the form of fractions of the stiffness of the solid embedded foundation. The variation of these results with $\mathfrak{J}$ is plotted in Fig. 2.

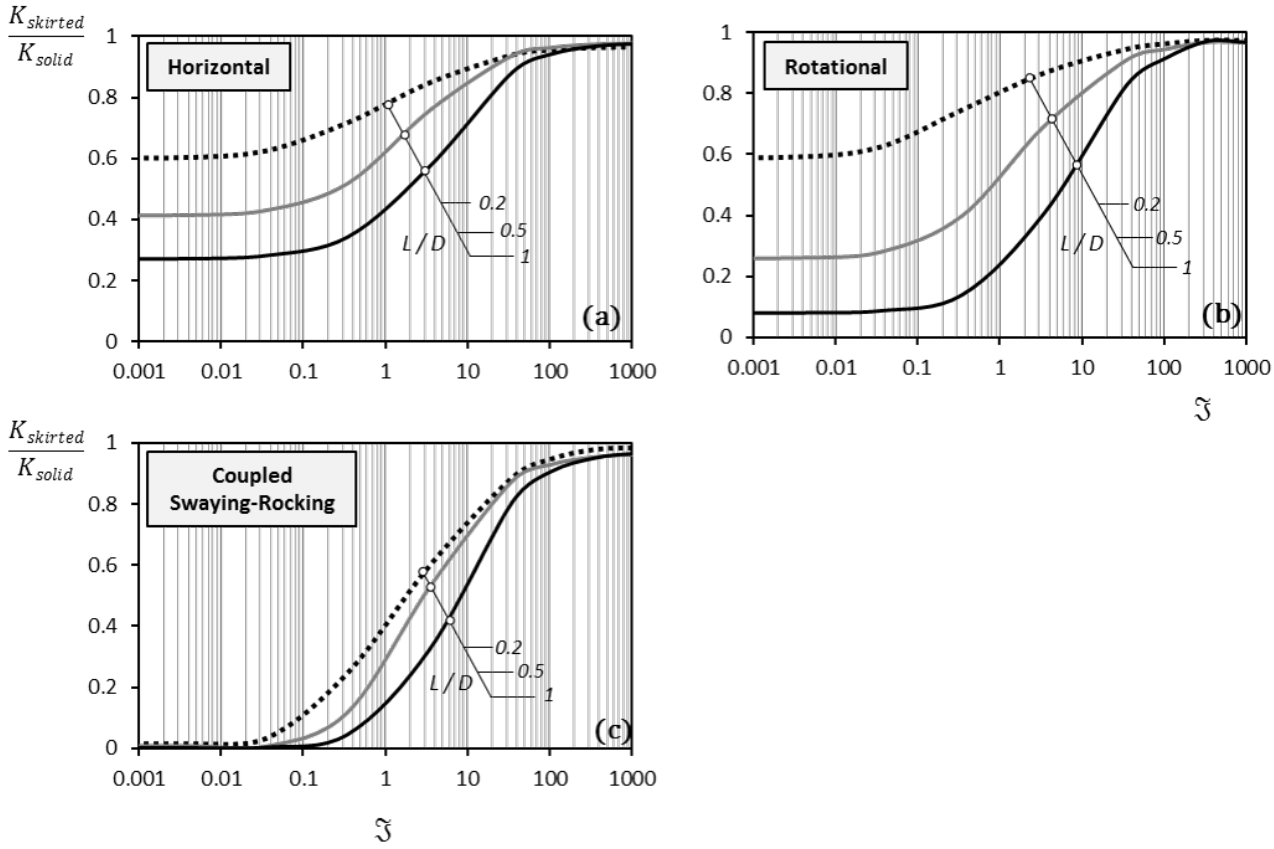

Figure 2. Ratios of the elastic stiffness of a skirted foundation over the elastic stiffness of the equivalent solid foundation versus $\Im$: (a) horizontal; (b) rotational and (c) coupled swaying-rocking.

It was found that the curves produced can be approximated by the following function:

$$\mathcal{S}(\mathcal{p}) = \frac{\mathrm{K_{skirted}}}{\mathrm{K_{solid}}} = \frac{\mathrm{K_{surf}}}{\mathrm{K_{solid}}} + \frac{\mathcal{p}\,\frac{\mathrm{K_{rigid}}-\mathrm{K_{surf}}}{\mathrm{K_{solid}}}}{1+\mathcal{p}} \tag{7}$$

$$\mathcal{p}\left(\Im, \frac{\mathrm{L}}{\mathrm{D}}\right) = \mathrm{a}\left(\frac{\mathrm{L}}{\mathrm{D}}\right)^{-\mathrm{b}} \Im^{\,\mathrm{c}} \tag{8}$$

where a, b, c factors varying for each type of stiffness, $K_{skirted}$ the stiffness of the flexible skirted foundation, K_{surf} the stiffness of the equivalent surface foundation, K_{solid} the stiffness of the equivalent solid embedded foundation and K_{rigid} the stiffness of the equivalent rigid skirted foundation. It can be considered as a simplification for the embedment values of interest ($L/D \leq 1$) that $K_{rigid} \approx K_{solid}$. Table 3 presents the values for factors a, b, c for each type of stiffness as well as the maximum error between the Equation 7 and the finite element analysis results.

Table 3. Coefficient values and maximum error for Equation

	a	**b**	**c**	**Error**
K_V	0.9	0.5	0.85	1.4%
K_H	0.3	0.75	0.8	1.8%
K_R	0.25	1	0.8	3.4%
K_C	0.2	0.7	0.85	5.6%
K_T	0.85	0.85	0.85	2.7%

EFFECT OF IMPERFECT INTERFACES ON THE RESPONSE OF SKIRTED FOUNDATIONS

The elastic stiffness coefficients of the soil-foundation system can only be considered approximately correct in the small-strain domain. For large displacements or rotations, geometric and material nonlinearities start to affect its response and the expressions derived previously are no longer applicable. Thus, it is important that the behaviour of the system be investigated as it enters the plastic domain and soil yielding, sliding and even uplift govern its response. Charts for the stiffness degradation of skirted foundations were produced with which the stiffnesses of the system could be appropriately reduced for the level of displacement or rotation imposed to the foundation and emphasis is given on the effect of interfaces on the initial stiffness of the system as well as on the ultimate capacity. In this section, only results for the horizontal, rotational and cross-coupling stiffness coefficients will be presented, since the more concerning issues for offshore wind turbines are those of lateral loading, either due to the combination of wind and wave loading or due to seismic excitation.

Horizontal Translation (without rotation)

Figure 3 compares the horizontal stiffness, as well as the maximum lateral capacity of rigid suction caissons, when imperfect interfaces between the skirts and the surrounding soil are implemented. Apparently, by introducing geometrical non-linearity, the initial stiffness of the system decreases from its "elastic value", as indicated in the vertical axis of the left charts. Note that the values of these charts has been divided by the elastic stiffness for the full contact conditions. When the soil-outer skirt interface has zero shear resistance (frictionless scenario), the initial stiffness reduction may be of the order of 25% compared to that under full contact conditions. Perhaps contrary to the reader's first anticipation, for the case of tensionless interface (where soil detachment is permitted) the initial horizontal stiffness of the system is slightly affected. The latter is attributed to the fact that the contribution of the sidewall that is normal to the vectorial load direction, in the overall stiffness is quite insignificant (it can be viewed as nothing more than a rectangular footing at the edge of a homogeneous quarter-space which is loaded perpendicular to its surface) compared to the one of the parallel to the loading direction sidewalls, which mainly act with shear stresses. Hence, the detachment of the former in the tensionless scenario (rough in shear but with zero tensile capacity) cancels only a small proportion of the overall stiffness. On the contrary, when frictionless interfaces are introduced, the zero shear resistance annuls the participation of the sidewalls that are parallel to the loading direction and the reduction of the total stiffness of the system is further distinguishable.

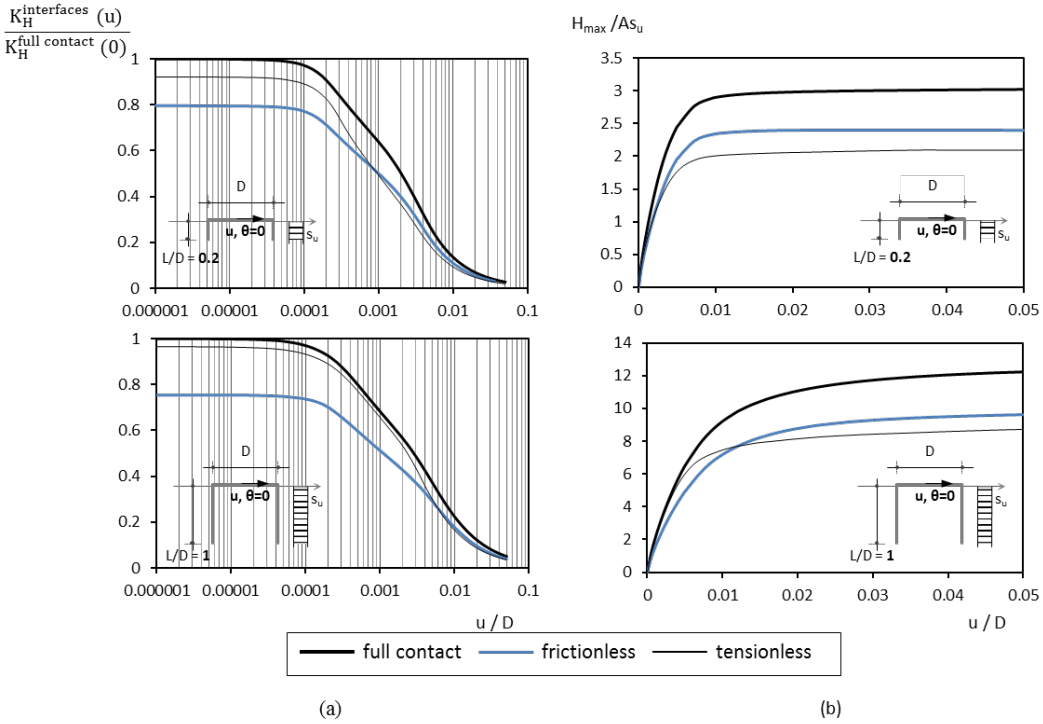

Figure 3. Effect of interface conditions on (a) the horizontal stiffness and (b) the maximum lateral capacity of rigid skirted foundations with embedment ratio 0.2 and 1.

Interestingly, the reversed effect is observed when the maximum horizontal capacity is examined (Fig. 3(b)). For the tensionless scenario a maximum horizontal capacity of 0.70 of the capacity under full contact conditions is reached, approximately 15% smaller than the corresponding under frictionless interfaces. At failure, the sidewalls that are parallel to the load direction experience shear stresses, thus providing less resistance than the sidewalls normal to the direction of loading, which act with passive and active normal stresses. Consideration of a tensionless boundary between the caisson and the soil is accompanied by the formation of a clear gap opposite to the direction of loading, and thereby the maximum capacity decreases more significantly.

Rotation (without translation)

The same procedure as above was carried out for the rotational stiffness derived from imposed rotation at the center of the rigid caisson lid with zero horizontal displacement. Figure 4 compares the rotational stiffness as well as the maximum moment capacity among the three interface assumptions. The same trend as for the horizontal stiffness is generally observed. Under the frictionless interface regime the initial stiffness of the soil-foundation system remains remarkably lower (almost 35%) than that under fully bonded conditions, while for the tensionless scenario the initial stiffness reduction is of the order of 10%.

A simple explanation of the relatively increased effect on this mode of loading could be obtained from the previous discussion: now, the two sidewalls that are orthogonal to the (vectorial) direction undergo a torsional-type movement about the horizontal axis passing from the center of the lid. Simultaneously, the two sidewalls that are parallel to the vectorial direction undergo a movement which can be de-composed into a vertical and a horizontal translation of their center, equal to $\theta D/2$ and $\theta L/2$, respectively, and rotation θ around their centroidal horizontal axis (rocking). Of these, the vertical movement invokes shear resistance (contributing by K_H), the horizontal movement invokes normal stresses (contributing by K_V) and the rotational mode invokes mainly normal stresses (contributing by K_R). Any footing subjected to moment loading affects only a limited volume of soil; in the traditional geotechnical jargon, it produces elastic “stress bulbs” of very limited extent. In contrast, force loading (in shear or normal mode) produces stress bulbs that go much deeper. But smaller affected area means smaller total displacements-rotations, and therefore larger stiffnesses. Hence, the sidewalls in rotational modes exhibit much greater stiffness than in translational modes, thus justifying the increased reduction due to imperfect interfaces. Finally, considering that torsional loading produces shallower stress bulbs than moment loading, as well as that an amount of shear resistance is provided also by the sidewalls that are parallel to the vectorial direction of loading (through their horizontal movement), not surprisingly the frictionless scenario results once more in further reduced initial stiffnesses compared to the tensionless interfaces.

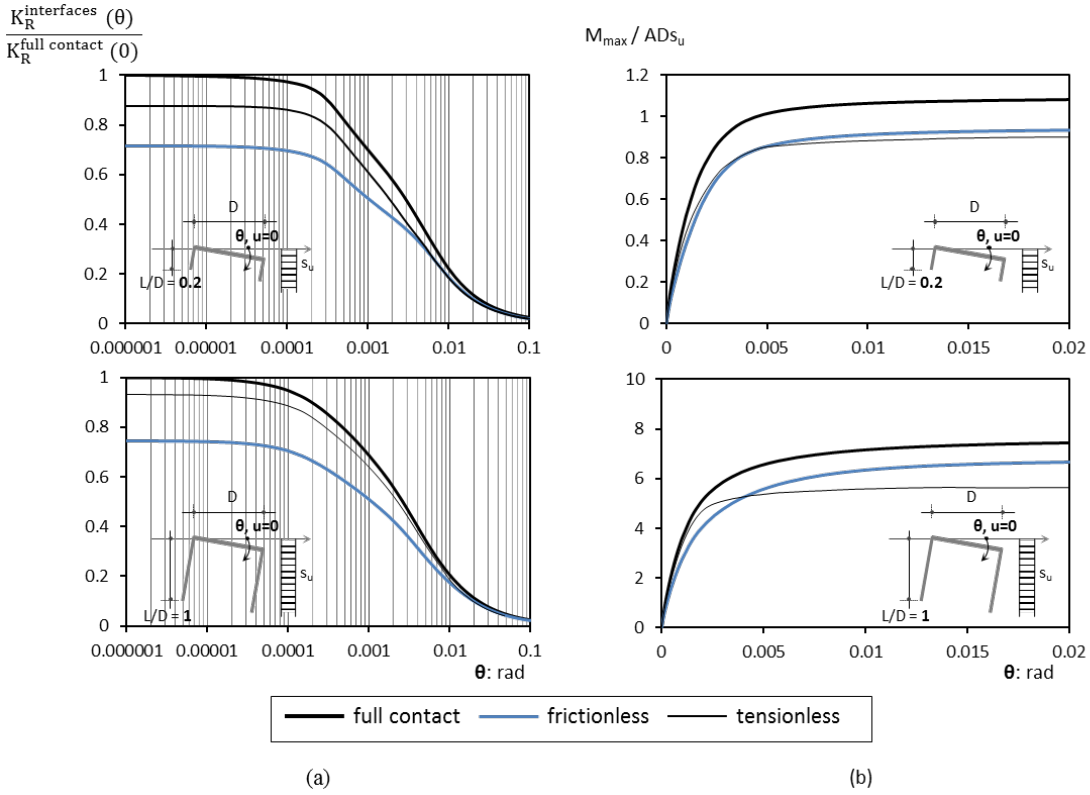

Figure 4. Effect of interface conditions on (a) the rotational stiffness and (b) the maximum moment capacity of rigid skirted foundations with embedment ratio 0.2 and 1.

As far as the maximum moment capacity is concerned, although frictionless interfaces produce less decreased capacity compared to the translation mode, owing to the more significant contribution of the caisson lid as stated previously, the chasm between the two imperfect-interface scenarios is now magnified with increasing embedment ratio. For the shallow case, the tensionless scenario reveals lower resistance than the frictionless one merely by 3%, with this discrepancy being more conspicuous for the deeply embedded caisson, reaching almost 20%, as depicted in Fig. 4(b).

Coupled swaying-rocking stiffness

Horizontal and moment loading on an embedded foundation engender a complex response that cannot be considered as a superposition of the two above load types, but rather as a coupled reaction. It reflects the development of horizontal reactions when rotation is applied to the foundation, owing to the embedment and the effect of lateral soil pressures. Therefore, it calls for investigation of the coupled swaying-rocking stiffness of the soil-foundation system, which has been derived from analyses with zero imposed displacement and rotation until failure.

Results are presented for the coupled swaying-rocking stiffness in Fig. 5 for the two extreme embedment ratios. The “bumps” present in the curves reflect the shaping of new failure zones beneath, around and within the skirts as they temporarily relieve the ones already formed due to excess displacements/rotations. The reader is encouraged to observe two key trends:

(a) with increasing embedment ratio, the initial cross-coupling stiffness for frictionless interfaces tends to decrease. This means that for shallow skirted foundations, zero shear resistance results in larger negative horizontal force to be applied in order to accumulate the same rotation. In other words, when an overturning moment (M) is applied in combination with a horizontal load (H), rotation due to coupling effect constitutes a larger amount of the overall angle of rotation compared to the ideal case of full contact, although the latter produces smaller total rotation in absolute values.

(b) with increasing embedment ratio the initial cross-coupling stiffness for the tensionless scenario has the tendency to increase. In the case of L/D=0.2, it is 10% smaller than the corresponding for full contact conditions (remaining lower than that for the frictionless scenario). However, for L/D=1 it

exceeds the value of the frictionless counterpart, but still remaining at 5% lower than the full contact case..

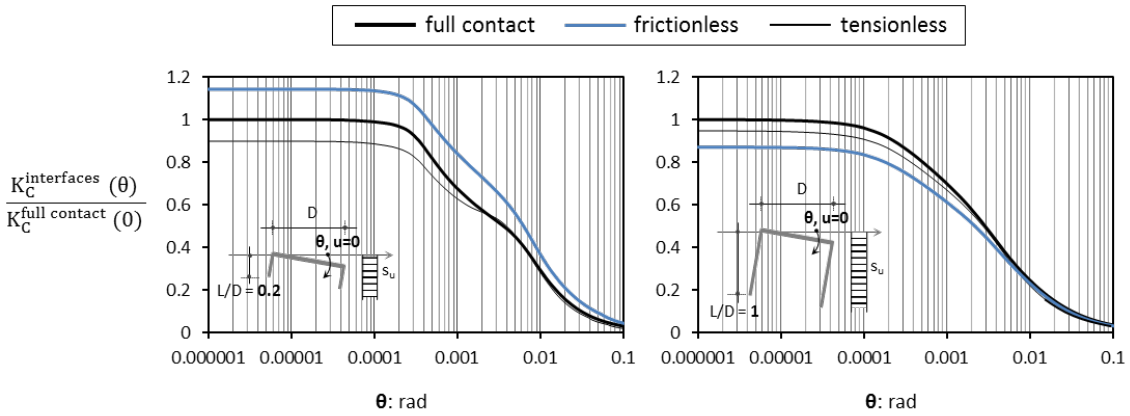

Figure 5. Effect of interface conditions on the coupled swaying-rocking stiffness of rigid skirted foundations with embedment ratio 0.2 and 1.

EFFECT OF SKIRT FLEXIBILITY ON NONLINEAR ROCKING STIFFNESS

Having defined the effect of imperfect interfaces on the nonlinear stiffnesses of rigid skirted foundations, this section explores the non-linear stiffness degradation when the skirt flexibility is introduced. Fig. 6 compares the nonlinear rocking stiffnesses among skirted foundations with different flexibilities for the two extreme embedment ratios (0.2 and 1). In the same diagram results for the solid embedded caisson (grey solid line) are presented for comparative purposes. Differences of the stiffness degradation among the three foundation types are barely distinguishable for the low L/D case. With increasing L/D, the more significant skirt contribution to the overall stiffness of the system escalates the discrepancy attributed to the skirts' flexibility, since the stiffness of the flexible alternative seems to decline less rapidly from its initial value. It is worth noting at this point that the absolute initial stiffness reduces with skirt flexibility and with imperfect interface assumptions, as proved in the previous sections. The normalization has been made with the respective initial stiffnesses; hence, all charts start from the value of 1.

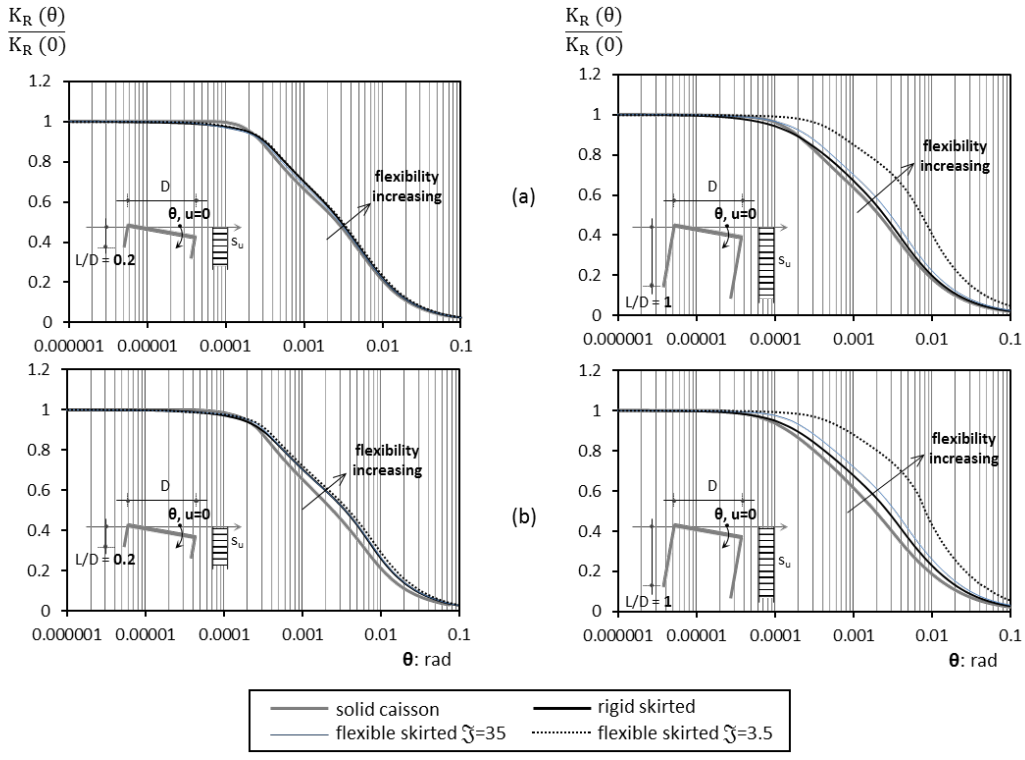

Figure 6. Non-linear rotational stiffness: effect of caisson flexibility under (a) full contact conditions and (b) frictionless interfaces for a shallow (L/D=0.2-left) and a deeply embedded foundation (L/D=1-right)

CONCLUSIONS

This paper has investigated the stiffness of the soil-suction caisson foundation system both in the elastic domain and when nonlinearities are considered, based on three-dimensional finite element analyses. Proper modifications of expressions from the literature were proposed to identify the elastic stiffness matrix of a solid embedded foundation with the load reference point at its top. Following, expressions for the stiffness components of flexible skirted foundations were engendered for variations in the characteristics of the system normalized by a parameter that produced unique stiffness values.

The second part of this study involved the investigation of the stiffness of the system in the large-strain domain and emphasis was given to the effect of imperfect soil-sidewalls interfaces, but a preliminary comparison among skirted foundations with different flexibilities has also been addressed. Consideration of frictionless interfaces allows sliding of the caisson from the soil, thus producing decreased stiffnesses, even for relatively small imposed displacements and rotations compared to the ideal case of full contact. On the other hand, tensionless interfaces, where detachment of the caisson from the soil is the prevailing mechanism, result in rather insignificant decrease of the initial stiffness of the system, although they proved more crucial in terms of maximum lateral and moment capacity. The observed trends were interpreted with simple soil-mechanics terms. Corresponding charts were produced that showed the reduction in the stiffness components with increasing displacements and rotations, giving the ability of estimating with an iterative procedure the true displacement and rotation of the foundation for different levels of imposed horizontal and moment loads.

REFERENCES

Anastasopoulos I., Gelagoti F., Kourkoulis R., & Gazetas G., (2012). Simplified Constitutive Model for Simulation of Cyclic Response of Shallow Foundations: Validation against Laboratory Tests. Journal of Geotechnical and Geoenvironmental Engineering, ASCE, 137, No. 12, 1154-1168.

Barari, A. & Ibsen, L. B. (2012). Undrained response of bucket foundations to moment loading. Appl. Ocean Res. 36, 12-21.

Bransby, M.F. & Randolph M.F. (1998).Combined Loading of Skirted Foundations. Géotechnique 48, No. 5, 637−655

Bransby, M. F. & Yun, G. J. (2009). The undrained capacity of skirted strip foundations under combined loading. Geotechnique 59, No. 2, 115-125

Byrne, B. W. (2000). Investigations of suction caissons in dense sand. DPhil thesis. Univ. of Oxford, Oxford, England.

Clukey, E. C. & Morrison, J. (1993). A centrifuge and analytical study to evaluate suction caissons for TLP applications in the Gulf of Mexico. In Design and Performance of Deep Foundations: Piles and Piers in Soil and Soft Rock, ASCE Geotechnical Special Publication, vol. 38, pp. 141-156. Reston, VA, USA: American Society of Civil Engineers.

Doherty, J. P. & Deeks, A. J. (2003). Elastic response of circular footings embedded in a non-homogeneous half-space. Geotechnique 53, No.8, 703-714.

Doherty, J.P. & Deeks, A. J. (2005), Adaptive coupling of the finite-element and scaled boundary finite-element methods for non-linear analysis of unbounded media. Computers and Geotechnics 32, No. 6, pp. 436-444.

Doherty, J. P., Houlsby, G. T. & Deeks, A. J. (2005). Stiffness of flexible caisson foundations embedded in nonhomogeneous elastic soil. Journal of Geotechnical and Geoenvironmental Engineering, ASCE 131, No. 12, 1498-1508.

Gazetas, G. (1983). Analysis of machine foundation vibrations: state of the art, Soil Dynamics and Earthquake Engng 2, No. 1, 2-42.

Gazetas, G. (1987). Simple physical methods for foundation impedances, Dynamics of Foundations and Buried Structures, Benerjee PK and Butterfield R., editors, Elsevier Applied Science, Chapter 2, 44-90.

Gazetas, G. (1991). Formulas and charts for impedances of surface and embedded foundations, Journal of Geotechnical Engineering, ASCE 117, No. 9, 1129–1141.

Gourvenec, S. (2007). Failure envelopes for offshore shallow foundations under general loading. Géotechnique 57, No. 9, 715–728.

Gourvenec, S. (2008). Effect of embedment on the undrained capacity of shallow foundations under general loading, Geotechnique 58, No. 3, 177–185.

Gourvenec, S., Acosta-Martinez, H. E. and Randolph, M. F. (2009). Experimental study of uplift resistance of shallow skirted foundations in clay under transient and sustained concentric loading, Geotechnique 59, No. 6, 525–537.

Gourvenec, S. and Barnett, S. (2011). Undrained failure envelope for skirted foundations under general loading. Geotechnique 61, No. 3, 263-270.

Houlsby, G. T., Kelly, R. B., Huxtable, J., & Byrne, B. W. (2005). Field trials of suction caissons in sand for offshore wind turbine foundations. Géotechnique 55, No. 4, 287–296.

Kourkoulis, R. S., Lekkakis, P. C., Gelagoti, F. M. & Kaynia, A. M. (2014). Suction caisson foundations for offshore wind turbines subjected to wave and earthquake loading: effect of soil-foundation interface. Geotechnique 64, No. 3, 171-185.

Liingaard, M., Andersen, L., Ibsen, L.B. (2007) Impedance of flexible suction caissons. Earthquake Engng Struct. Dyn 36, No. 14, 2249 - 2271.

Poulos, H. G. and Davis, E. H. (1974). Elastic solutions for soil and rock mechanics, published by John Wiley & Sons, Inc., New York, London, Sydney, Toronto.

Roesset, J. M. (1980). Stiffness and damping coefficients of foundations. Dynamic Response of Foundations: Analytical Aspects, M.W. O' Neil and R. Dobry (eds), ASCE, 1-30.

Taiebat, H.A. and Carter, J.P. (2000). Numerical studies of the bearing capacity of shallow foundations on cohesive soil subjected to combined loading. Geotechnique 50, No. 4, 409-418.

Tani, K. & Craig, WH. (1995). Bearing capacity of circular foundations on soft clay of strength increasing with depth. Soils and Foundations 35, No. 2, 37-47.

Ukritchon, B., Whittle, A. J. and Sloan, S. W. (1998). Undrained limit analyses for combined loading of strip footings on clay, J. Geotech. Geoenviron. Engng, ASCE 124, No. 3, 265-276.

Vulpe, C. (2015). Design method for the undrained capacity of skirted circular foundations under combined loading: effect of deformable soil plug. Géotechnique 65, No. 8, 669–683.